Brain Struct Funct
DOI 10.1007/s00429-013-0573-z

ORIGINAL ARTICLE

The differential effects of acute right- vs. left-sided vestibular failure on brain metabolism

Sandra Becker-Bense · Marianne Dieterich · Hans-Georg Buchholz · Peter Bartenstein · Mathias Schreckenberger · Thomas Brandt

Received: 18 October 2012 / Accepted: 3 May 2013

Abstract The human vestibular system is represented in the brain bilaterally, but it has functional asymmetries, i.e., a dominance of ipsilateral pathways and of the right hemisphere in right-handers. To determine if acute right- or left-sided unilateral vestibular neuritis (VN) is associated with differential patterns of brain metabolism in areas representing the vestibular network and the visual–vestibular interaction, patients with acute VN (right $n = 9$; left $n = 13$) underwent resting state ^{18}F-FDG PET once in the acute phase and once 3 months later after central vestibular compensation. The contrast acute vs. chronic phase showed signal differences in contralateral vestibular areas and the inverse contrast in visual cortex areas, both more pronounced in VN right. In VN left additional regions were found in the cerebellar hemispheres and vermis bilaterally, accentuated in severe cases. In general, signal changes appeared more pronounced in patients with more severe vestibular deficits. Acute phase PET data of patients compared to that of age-matched healthy controls disclosed similarities to these patterns, thus permitting the interpretation that the signal changes in vestibular temporo-parietal areas reflect signal increases, and in visual areas, signal decreases. These data imply that brain activity in the acute phase of right- and left-sided VN exhibits different compensatory patterns, i.e., the dominant ascending input is shifted from the ipsilateral to the contralateral pathways, presumably due to the missing ipsilateral vestibular input. The visual–vestibular interaction patterns were preserved, but were of different prominence in each hemisphere and more pronounced in patients with right-sided failure and more severe vestibular deficits.

Keywords Vertigo · Vestibular system · PET · Vestibular neuritis · Visual–vestibular interaction

Abbreviations

BA	Brodmann area
^{18}F-FDG-PET	Fluoro-deoxyglucose positron emission tomography
CMRglc	Cerebral metabolic rate of glucose consumption
SVV	Subjective visual vertical
VN	Vestibular neuritis
VOI	Volume of interest

S. Becker-Bense and M. Dieterich contributed equally as first authors.

S. Becker-Bense (✉) · M. Dieterich
Department of Neurology, Ludwig-Maximilians-University Munich, Marchioninistrasse 15, 81377 Munich, Germany
e-mail: sandra.bense@med.uni-muenchen.de

S. Becker-Bense · M. Dieterich · P. Bartenstein · T. Brandt
The German Center for Vertigo and Balance Disorders (IFB-LMU), University of Munich Hospital, Munich, Germany

M. Dieterich · P. Bartenstein
Munich Cluster for Systems Neurology (SyNergy), Munich, Germany

H.-G. Buchholz · M. Schreckenberger
Department of Nuclear Medicine, Johannes Gutenberg-University, Mainz, Germany

P. Bartenstein
Department of Nuclear Medicine, Ludwig-Maximilians-University Munich, Munich, Germany

T. Brandt
Institute of Clinical Neuroscience, Ludwig-Maximilians-University Munich, Munich, Germany

Published online: 18 May 2013

Introduction

Human fMRI and PET studies have revealed the existence of a network of areas in the temporo-parietal cortex of both hemispheres which processes vestibular information during vestibular stimulation. Its core region is the parieto-insular vestibular cortex (Bense et al. 2001; Fasold et al. 2002; Emri et al. 2003; Naito et al. 2003; Stephan et al. 2005; Miyamato et al. 2007; Schlindwein et al. 2008; Zu Eulenburg et al. 2012). A similar region was defined earlier in electrophysiological and tracer studies on non-human primates (Akbarian et al. 1994; Guldin and Grüsser 1996; Chen et al. 2010). The activation pattern is asymmetrical, primarily occurring in right-handers in the right hemisphere (Naito et al. 2003; Dieterich et al. 2003) and in the ipsilateral ascending vestibular pathways (Bense et al. 2003; Dieterich et al. 2003). During vestibular stimulation signal decreases occur simultaneously within visual and somatosensory cortex areas, and vice versa (Wenzel et al. 1996; Brandt et al. 1998; Bense et al. 2001; Naito et al. 2003; Stephan et al. 2005). This pattern of signal increases and decreases—also seen between the somatosensory, nociceptive, and visual systems (Bense et al. 2001; Lauri-enti et al. 2002; Maihöfner et al. 2006; Merabet et al. 2007)—led to the hypothesis that there is a fundamental reciprocal inhibitory interaction between the sensory systems at the cortical level (Brandt et al. 1998). Such inhibitory sensory interactions can prevent perceptual confusion when multimodal inputs are contradictory. In other words, the stimulation of a single peripheral cranial nerve, such as the vestibular nerve, is able to elicit complex (bottom-up) processes in different sensory cortical systems, i.e., there is a specific, bilateral "activation–deactivation" pattern within the cortex.

The simultaneous modifications of different sensory systems might have originated from the need for protection. Since stimulation of the peripheral vestibular nerve or labyrinth results not only in rotatory vertigo but also in vestibular nystagmus with blurred vision, it would be helpful if the sensitivity of the visual system were decreased in this situation by a "deactivation" of the neurons of the visual cortex bilaterally (Wenzel et al. 1996; Bense et al. 2001; Naito et al. 2003; Stephan et al. 2005; Schlindwein et al. 2008). Indeed, significant impairment of visual functions has been found during psychophysical investigations of high-resolution visual mental imagery and mental rotation tasks performed by healthy subjects during vestibular caloric stimulation (Mast et al. 2006).

Both unilateral vestibular stimulation, on the one hand, and unilateral failure of the vestibular end organ, on the other, create a vestibular tonus imbalance, but from opposite premises: a unilateral stimulation increases the resting discharge input from one end organ, whereas a unilateral lesion reduces it. The direction of signs and symptoms of the excitation as opposed to the lesion of the conduction block are thus opposite. The pattern in healthy subjects during unilateral vestibular stimulation should be comparable to that of patients with unilateral vestibular loss and might include areas similar to the pattern of the unaffected ear. A pilot PET study with five right-handed patients with acute right-sided vestibular neuritis (VN) (Bense et al. 2004) indeed showed similarities and raised the question of whether left-sided VN due to the above-described two-organizational asymmetries causes different brain activation patterns. In that study regional cerebral glucose metabolism was significantly increased in the acute stage of VN in temporo-parietal multisensory vestibular areas of the left hemisphere.

In the current ^{18}F-FDG PET study we analyzed the differential effects of acute right- and left-sided VN in right-handers (right-sided VN, $n = 9$; left-sided VN, $n = 13$) on the vestibular network in the two hemispheres and on the visual-vestibular interaction with respect to hemispheric dominance in the acute stage and 3 months later after central vestibular compensation had occurred. The following questions were of special interest: (a) does the acute lesion-induced vestibular tonus imbalance between the two labyrinths lead to modulation of neural activity within the thalamo-cortical vestibular system, which differs depending on the ear affected, the vestibular "dominant" right ear or the vestibular "non-dominant" left ear? (b) Which determinants can best explain the differences: the subjects' handedness or the side of the lesioned ear, or both? (c) Does the acute lesion-induced vestibular tonus imbalance cause modulation of the signal decreases within the visual and somatosensory systems, and if so, is this pattern different for right- and left-sided lesions? (d) If there is a difference in the patterns of patients with right- and left-sided VN, does this include other areas not normally involved in the vestibular processing of healthy subjects during vestibular stimulation?

Methods

Patients

Nine right-handed patients with acute right-sided VN (4 males, 5 females; ages 41–76 years, mean age 61.2 ± 9.8 years) and 13 right-handed patients with acute left-sided VN (7 males, 6 females; ages 42–80 years, mean age 60.7 ± 13.0 years) participated. All had a spontaneous horizontal-rotatory nystagmus of 5–20°/s mean slow phase velocity (right 7.3°/s, left 11.8°/s). Six patients in the two groups did not respond to caloric testing on the affected side (complete paresis of the horizontal semicircular canal,

100 % asymmetry); the others had incomplete deficits with a mean asymmetry of 74.6 % in right- and 66.0 % in left-sided VN. In all the subjective visual vertical (SVV) was tilted ipsilaterally between 5° and 25° (12.6° right, 7.5° left). The SVV was more tilted in the subgroups with the most severe vestibular deficits (14.1° right; 9.3° left). The first PET scan was acquired between days 1 and 14 after symptom onset (median: 6.8 right, 6.3 left). None of the patients showed signs of relevant central vestibular disorders.

Three months later all patients were symptom-free without spontaneous nystagmus or SVV tilts (analogous findings in Halmagyi et al. 2010). Caloric testing revealed complete recovery (<10 % asymmetry) in eight patients (3 right, 5 left). Only one patient in each group had a persisting, complete paresis. The remaining patients showed median asymmetries of 37 % for right-sided and 38 % for left-sided VN. Thus, when all the vestibular parameters were considered together, there was no statistical difference between right- and left-sided VN.

All patients were strongly right-handed based on a laterality quotient for handedness of +100 or +80 according to the 10-item inventory of the Edinburgh test (Oldfield 1971). None of the patients had a relevant physical illness, in particular no cochlear, vestibular, or central nervous system disorders. None were on centrally active medication or vestibular sedatives. The study was carried out in accordance with the Helsinki Declaration and was approved by the local ethics committee and the radiation protection authorities. All patients gave their informed written consent.

Neurological, neuro-orthoptic, neurophysiological testing

Diagnosis was based on the occurrence of the chief symptoms, a careful neurological and neuro-otological examination including neuro-orthoptic analysis (Baloh 2003), after exclusion of central neurological disorders. Clinical examination included fundus photography (to detect tonic vestibular disorders such as skew deviation or ocular torsion), measurements of the SVV to determine the degree of tonus imbalance in the roll plane (Brandt and Dieterich 1994), and binocular electro-oculography (direct current) recording with caloric testing. In accordance with Honrubia (1994) vestibular paresis was defined as >25 % asymmetry between the right- and the left-sided responses; this was calculated with the formula of Jongkees et al. (1962) based on the slow-phase velocity: $\{[(R\ 33° + R\ 44°) - (L\ 30° + L\ 44°)]/[(R\ 30° + R\ 44° + L\ 30° + L\ 44°)]\} \times 100$. High-resolution MRI was performed in a 1.5 standard clinical scanner (Siemens, Germany) using axial T1-weighted spin-echo imaging; T2-weighted turbo spin-echo and/or diffusion-weighted sequences excluded pseudoneuritis of the vestibular nucleus or vestibular afferents within the brainstem.

PET examination, image reconstruction, statistical analysis

Each patient underwent two PET scans of 150 ± 20 MBq ^{18}F-fluoro-deoxyglucose (^{18}F-FDG) in an ECAT Exact PET Scanner (Siemens/CTI, Knoxville) under standardized conditions (Bartenstein et al. 2002): (a) first in the acute stage of VN (acute phase: median on day 6.5 after symptom onset) and (b) 3 months later in the stage of central compensation (chronic phase). The two examinations were performed at the same time of the day to minimize influences of circadian variability of cerebral glucose metabolism (Bartlett et al. 1988). On the examination day patients were asked to fast for at least 8 h before the PET study, but allowed free access to unsweetened drinks. ^{18}F-FDG was administered intravenously while the patients lay in a quiet and darkened room with their eyes closed and followed the instruction to relax. To obtain transaxial images approximately parallel to the intercommissural line (AC–PC line), the patient was positioned on the scanner's bed with the canthomeatal line parallel to the detector rings.

The emission scan started 30 min after 18-FDG injection and continued for 20 min in a three-dimensional acquisition mode. The patients remained in one bed position, since the PET scanner has an axial field of view of 16.2 cm covering the whole brain. Attenuation correction was calculated using a computerized threshold limit routine to define an iso-intensity contour of the maximum cerebral activity/pixel. The exact position of an iso-intensity density contours was controlled visually slice-by-slice and eventually corrected manually. Forty-seven transversal slices, each 3.375-mm thick, were reconstructed using filtered back projection with a ramp and a 4-mm Hanning filter. The images had a transaxial resolution of 6.0 mm in the center of the field-of-view with full width at half maximum (FWHM) (Wienhard et al. 1992).

Three-dimensional stereotactic surface projections of the individual datasets as well as parametric *Z*-score images were generated in a standardized manner in order to compare each individual subject's data with a normal reference database consisting of 21 normal controls using NEUROSTAT (University of Michigan) as described earlier (Bartenstein et al. 1997, 2002). By applying this latter procedure, as is usually done in clinical FDG-PET diagnostics, it was possible to exclude pathological cerebral glucose uptake patterns typical for neurodegenerative disorders such as Alzheimer's disease or other central nervous system disorders.

Further statistical analysis of the data was done using Statistical Parametric Mapping software (Wellcome Department

of Cognitive Neurology, London, UK, http://www.fil.ion.ucl.ac.uk/spm). The PET images were realigned, spatially normalized into the standard anatomical space (Friston et al. 1995a) defined by an FDG template according to Gispert et al. (2003) by means of linear and non-linear transformations and smoothed with a three-dimensional Gaussian filter using a 12-mm FWHM. The effect of the two different stages of VN on regional cerebral 18-FDG activity was estimated according to the general linear model (Friston et al. 1995b). After proportional scaling of all scans to mean global cerebral activity (Friston et al. 1990), *t*-statistical parametric maps were calculated on a voxel-by-voxel basis using a pooled variance estimated from the whole-brain gray matter (Worsley et al. 1992); the values were expressed as *Z*-scores. The following analyses were performed: (1) categorical comparisons of two patients' PET scans at different stages of the disease by a paired *t* test (acute phase vs. chronic phase; chronic phase vs. acute phase), (2) statistical correlation analyses between FDG uptake in the acute phase of VN (first PET scan) and different parameters (e.g., degree of spontaneous nystagmus, SVV tilts, asymmetry of caloric testing (%), latency in days between symptom onset and first PET, and (3) statistical comparisons between both patient groups (left- and right-sided VN (multigroup two condition analyses; analyses of differences of differences): (A) (VN right acute–chronic phase) vs. (VN left acute vs. chronic phase); (B) (VN right chronic–acute phase) vs. (VN left chronic–acute phase). The categorical comparisons were calculated for the groups of patients with right-sided ($n = 9$) and left-sided VN ($n = 13$), as well as for each of the two subgroups with the most severe vestibular deficits (complete paresis $n = 6$) in the acute phase. For the correlation analyses the individual parameters belonging to each PET image were entered as covariates into the design matrix. Furthermore, age and gender as covariates were added to the regression analyses. This was done separately for patients with right- and left-sided VN, as well as for the pooled patient group. The multigroup analyses were done for the whole patient group ($n = 22$) as well as for the most severe cases ($n = 12$).

In a fourth analysis, the glucose metabolism in the acute phase of VN was compared to that of an age- and gender-matched control group in a complete resting state (scanned earlier under identical conditions) by group subtraction analyses. This additional statistical verification by a control group was useful, since only two FDG-PET scans were permitted for each subject. It allowed us to check the activation patterns induced by the vestibular tone imbalance per se (serving as substitution base line).

CMRglc foci were considered significant for $p \leq 0.001$ uncorrected and if larger than ten voxels according to the theory-driven a priori hypothesis for visual areas (Brandt et al. 1998; Kleinschmidt et al. 2002) and for vestibular areas (Brandt et al. 1998; Lobel et al. 1998; Bense et al. 2001, 2004; Dieterich et al. 2003; Stephan et al. 2005; Schlindwein et al. 2008), and based on the theory of random Gaussian fields (Lumer et al. 1998). These earlier functional imaging PET and fMRI studies in healthy volunteers used different vestibular stimulations such as galvanic (8th nerve stimulation), caloric irrigation (horizontal canal stimulation), or vestibular evoked myogenic potentials (otolith stimulation); all showed congruent results with signal increases in vestibular and decreases in visual cortical areas. During visual stimulation the pattern was inverted, showing signal increases in visual areas and decreases in vestibular areas.

For anatomical localization of clusters, the MNI coordinates were transformed into the Talairach space using the mni2tal tool provided by CBU Imaging wiki (http://imaging.mrc-cbu.cam.ak.uk). The nomenclature of the anatomical structures as well as defined anatomical landmarks follows (Talairach and Tournoux 1988; Naidich and Brightbill 2003; Yousry et al. 1997).

Results

Group analyses of acute phase (A) vs. compensated stage (B)

Right-sided vestibular neuritis

In the group analysis of the contrast A vs. B, significant clusters were seen in the central pontomesencephalic brainstem, which merged into the adjacent temporal lobes bilaterally including the lentiform nuclei and posterolateral vestibular thalami, as well as into the contralateral left posterior insula region and the right parahippocampal gyrus/uncus (Table 1; Figs. 1, 2). The left parahippocampal gyrus/uncus showed a separate activation cluster. Additional signal differences were located in the anterior cingulate gyrus (BA 32/24), right superior temporal gyrus (BA 38/47), and the caudate nucleus bilaterally.

In the contrast B vs. A, widespread clusters were seen in the visual cortex, the cuneus, fusiform, lingual, middle and inferior occipital gyri (BA 17, 18, 19) including lower parts of the left precuneus. Furthermore, both parietal cortices, the superior (BA 7) and inferior (BA 40) with parts of the postcentral gyrus showed signal differences. They represent multisensory vestibular and somatosensory areas (Table 1; Fig. 1). A smaller cluster was also found in the anterior cingulate gyrus (BA 24/31).

Left-sided vestibular neuritis

In the group analysis A vs. B, significant clusters were seen in the pontomesencephalic brainstem bilaterally, merging

Table 1 Categorical comparison of FDG-PET scans of nine patients with right-sided and 13 with left-sided VN in the acute stage with their repeat scan 3 months later after clinical recovery (paired *t* test)

Area	Function/BA	Side	Coordinates [*x*, *y*, *z*]	*Z*-score	Cluster size
(I) VN right: acute phase vs. chronic phase					
Lentiform nucleus	Basal ganglia	L	−12, −4, −6	5.40	2796
			−12, 2, 0	4.74	
Lentiform nucleus	Basal ganglia	R	10, 10, −4	4.61	
			14, 8, −2	4.21	
Brainstem ponto-mes., merging into dorsal thalamus	Oculomotor		8, −36, −12	3.98	
		L	−6, −18, 12	3.58	
		R	10, −6, −2	3.94	
Posterior insula	Vestibular	L	−32, −18, 0	3.08	
Uncus/parahippocampal g.	Limbic	R	30, −14, −14	4.22	
Uncus/parahippocampal g.	Limbic	L	−26, −2, −28	4.14	556
Anterior cingulate g.	BA 32/24	R	10, 44, 0	4.18	303
Superior temporal g.	BA 38/47	R	42, 14, −18	3.08	20
Caudate nucleus/gray matter		R	20, 2, 20	2.83	16
		L	−16, 8, 18	2.82	15
(II) VN right: chronic phase vs. acute phase					
Middle occipital gyrus/cuneus/lingual/inferior occipital/fusiform gyrus	BA 17/18/19 visual cortex	R	32, −86, 10	3.69	2704
			28, −94, 14	3.63	
			28, −92, −14	3.30	
Inferior occipital/fusiform/lingual/middle occipital gyrus/precuneus	BA 17/18/19 visual cortex	L	−22, −92, −8	3.58	1782
			−24, −88, −20	3.55	
			−26, −74, 18	3.11	
Superior parietal lobule/precuneus	BA 7	L	−28, −68, 54	4.44	1153
			−24, −58, 64	4.06	
Inferior parietal lobule/postcentral gyrus	BA 40 sensory	L	−56, −40, 44	4.20	
			−56, −40, 50	3.15	
Superior parietal lobule	BA 7	R	22, −60, 64	3.19	243
Inferior parietal lobule/postcentral gyrus	BA 40 sensory	R	62, −62, 44	3.08	142
			56, −32, 58	2.90	
Inferior parietal lobule/postcentral gyrus/transverse temporal gyrus	BA 40 sensory	R	36, −34, 42	3.81	505
			54, −24, 28	3.33	
			50, −28, 18	2.61	
Anterior cingulate gyrus	BA 24/31	L	−8, −12, 0	3.27	60
(III) VN left: acute phase vs. chronic phase					
Brainstem ponto-mes. merging into the cerebellar hemispheres and vermis bilaterally	Oculomotor	L	−4, −34, −14	4.31	3737
		R	6, −36, −6	3.61	
Posterior insula	Vestibular	R	32, −16, −8	4.46	
			46, −6, −8	3.61	
Lentiform nucleus	Basal ganglia	R	32, −12, 6	3.09	
Parahippocampal gyrus	Limbic	R	22, −4, −14	4.61	
Subcallosal/medial frontal/anterior cingulate gyrus	Limbic	L	−6, 12, −14	4.79	
Caudate/lentiform nucleus/gray matter	Basal ganglia	L	−22, −2, 20	3.22	156
			−24, −20, 20	3.02	
(para-)hippocampal gyrus	Limbic	L	−36, −34, 0	3.00	129
Anterior cingulate gyrus/subgyral frontal lobe	BA 31	R	20, −24, 38	2.95	37
Superior temporal gyrus	BA 38	R	40, 10, −24	2.76	67

Table 1 continued

Area	Function/BA	Side	Coordinates [*x*, *y*, *z*]	*Z*-score	Cluster size
(IV) VN left: chronic phase vs. acute phase					
Inferior occipital/fusiform g.	BA 18 visual cortex	L	−46, −82, −14	3.00	167
Middle frontal gyrus	BA 46/10	R	54, 44, 16	3.28	158
			36, 64, 10	2.92	
Precuneus	BA 19	L	−36, −88, 40	3.43	158
Precuneus	BA 7	R	6, −70, 62	3.00	62
Supramarginal gyrus/inferior parietal lobule	BA 40	L	−40, −44, 36	2.88	62

Brain areas showing signal increases (I) as well as decreases (II) are given with their maximum *Z*-scores, corresponding Brodmann areas (*BA*), coordinates, and cluster sizes ($p \leq 0.001$ uncorrected)

upward into the contralateral right posterior insula and retroinsular region, right parahippocampal gyrus, lentiform nucleus, and the adjacent subcallosal/medial frontal gyrus/white matter, and merging downward in both cerebellar hemispheres and the vermis bilaterally (Table 1; Figs. 1, 2). Within the left hemisphere, the caudate/lentiform nuclei and the (para)hippocampal gyrus formed separate activation clusters. Smaller activation clusters also occurred in the right superior temporal gyrus (BA 38) and the sub gyral anterior cingulate gyrus. This activation pattern appeared to be a mirror image of that observed in right-sided VN.

In the contrast B vs. A, smaller clusters were seen in the visual cortex, the left fusiform and inferior occipital gyri (BA 18), and bilaterally in the precuneus/inferior parietal lobule (BA 7, 19, 40). An additional cluster was located in the right middle frontal gyrus (BA 46/10). Areas were not found in the somatosensory cortex at $p < 0.005$. An area in the right inferior parietal lobule (BA 40) with its adjacent postcentral gyrus (somatosensory cortex) was seen only at $p < 0.01$. Thus, the clusters were fewer and smaller compared to those in right-sided VN, but showed a similar pattern.

Other sensory areas that are normally not involved in healthy subjects during vestibular stimulation were not found.

Subgroup analyses of acute phase (A) vs. compensated stage (B) in six patients with caloric unresponsiveness

Right-sided vestibular neuritis (n = 6)

Clusters were seen in the right anterior cingulate gyrus (BA 32/24), and symmetrically in the anterior pontomesencephalic brainstem and its adjacent lentiform nuclei, parahippocampal gyri, hypothalami and posterior thalami, on the right side bordering the retroinsular region (Table 1). A small cluster was found in the left superior temporal gyrus (BA 38).

The inverse contrast B vs. A showed large clusters bilaterally in the visual cortex, the cuneus, fusiform, lingual, inferior and middle occipital gyri (BA 17, 18, 19) (Table 1; Fig. 1). Other bilateral signal differences were located in the inferior parietal lobule (BA 40) and parts of the postcentral gyrus (somatosensory cortex) as well as in the superior parietal lobule/precuneus (BA 7). No signal differences were found in the brainstem and cerebellum.

Left-sided vestibular neuritis (n = 6)

In the group analysis A vs. B, a large cluster was found in the (medullary-ponto-) mesencephalic brainstem, which spread into the hypothalamus bilaterally and the right posterior thalamus (Table 1). Other signal differences were located in the basal ganglia (lentiform and caudate nucleus) bilaterally, right parahippocampal gyrus, right posterior insula, left anterior cingulum (BA 32), and the cerebellum bilaterally. In contrast to right-sided VN, most areas were located within the cerebellum and brainstem.

In the contrast B vs. A, signal differences occurred bilaterally in the visual cortex and right somatosensory cortex (postcentral gyrus) (Table 1; Fig. 1). These were more pronounced than those in the entire group of 13 patients with left-sided VN, but fewer than those in right-sided VN.

Correlation analyses of glucose metabolism with oculomotor and vestibular parameters

Slow-phase velocity of the spontaneous nystagmus

There was a significant positive correlation between slow-phase velocity of the spontaneous nystagmus in the acute stage of right-sided VN and the glucose metabolism for the anterior insula bilaterally (inferior frontal gyrus, BA 45, 47, 10; Fig. 3, left VOI 9: $T = 3.85$; right VOI 10: $T = 3.68$), the left posterior insula (VOI 11: $T = 3.55$), the left middle temporal gyrus (BA 37, 19; $T = 3.48$), the lateral left inferior frontal gyrus (BA 46; partly prefrontal cortex; $T = 4.92$; $R^2 = 0.67$), and the more dorsally located left inferior frontal/precentral gyrus (BA 6, 9; frontal eye field; $T = 4.15$; $R^2 = 0.0.59$). All represent multisensory

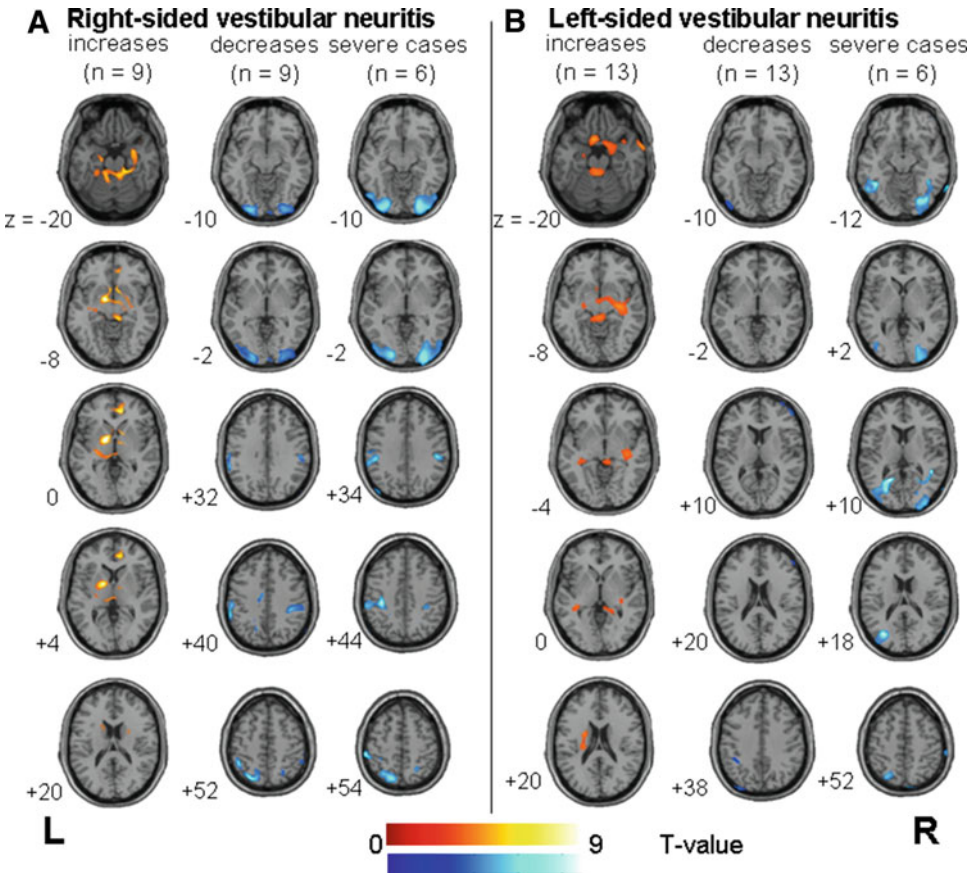

Fig. 1 **a** Statistical group analysis of nine right-handed patients with right-sided VN vs. the control condition 3 months later without any stimulation indicates significant signal changes ("activations" in *red*) in the contralateral left thalamus, the posterior insula merging with the lentiform nucleus as well as the right anterior cingulate gyrus and mesencephalon bilaterally ($p \leq 0.001$ uncorrected). Simultaneous signal decreases ("deactivations" in *blue*) were located in the visual and somatosensory cortex bilaterally. Statistical group analysis of the six patients with the most severe cases of right-sided VN showing similar signal decreases in the visual (BA 17/18/19) and somatosensory (BA 2/BA 40/2/3) cortex areas. **b** In the 13 right-handed patients with left-sided VN signal increases (*red*) were mainly found in the posterior insula, retroinsular region, and lentiform nucleus of the contralateral right hemisphere as well as in the mesencephalon and hippocampus bilaterally and the left-sided paraventricular white matter. Simultaneously signal decreases appeared in smaller clusters in the left fusiform and inferior occipital gyri and the precuneus/inferior parietal lobule bilaterally. Signal decreases were more pronounced in the group analysis of the six patients with the most severe left-sided VN than in the 13 patients, but there were fewer than in right-sided VN. This "activation–deactivation" pattern fits the concept of a reciprocal inhibitory intersensory visual–vestibular interaction found earlier during caloric vestibular stimulation in healthy volunteers. It further reflects the central vestibular tonus imbalance at cortical level, which is induced by the unilateral peripheral vestibular deficit

vestibular cortex or oculomotor areas. Furthermore, the eye muscles within the orbita showed a positive correlation with the nystagmic movements.

In left-sided VN patients slow-phase velocity correlated with glucose metabolism in the left middle frontal/precentral gyrus (BA 9; frontal eye field; VOI 12: $T = 5.02$), the left middle temporal gyrus (BA 21; $T = 3.53$), the left inferior parietal lobule (BA 40; $T = 3.81$), and the superior parietal lobule/precuneus bilaterally (Fig. 3; right: $T = 4.08$: left: $T = 3.58$; $R^2 = 0.50$).

The correlation analyses with the degree of spontaneous nystagmus in the acute phase for the pooled patient data gave no additional information. Analogous positively correlated clusters were seen in the multisensory vestibular cortex and oculomotor areas, e.g., the left inferior frontal/precentral gyrus (BA 9, 6, partly prefrontal cortex and frontal eye field), inferior parietal lobule (BA 40), middle temporal (BA 21, 22, 39), and middle occipital gyrus (BA 19, 37, motion-sensitive area MT/V5).

Analysis of neither the pooled data nor that for right- and left-sided VN separately gave significant negative correlations of the glucose metabolism with spontaneous nystagmus.

Tilts of the subjective visual vertical (SVV)

SVV tilts indicate the severity of tonic vestibular dysfunction in the acute phase (Curthoys and Halmagyi 1994).

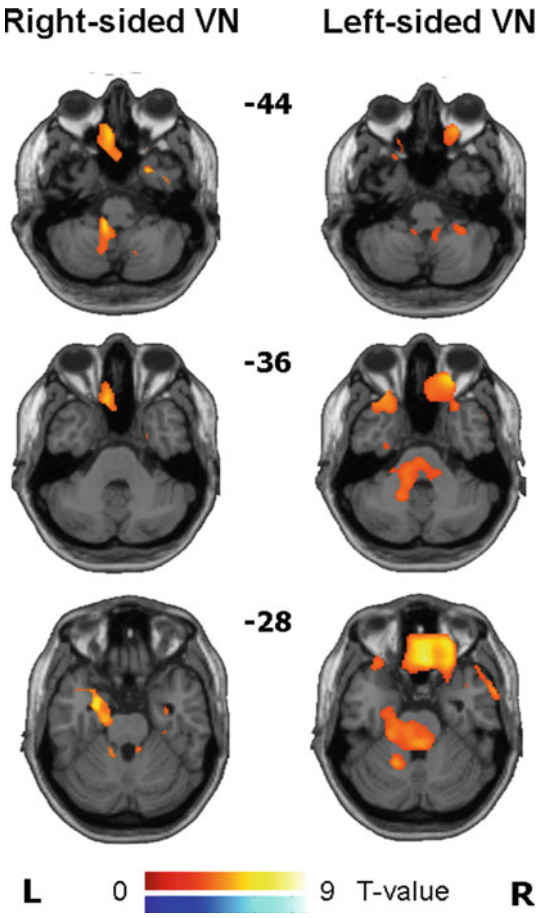

Fig. 2 Statistical group analysis of right-handed patients, nine with right-sided VN and 13 with left-sided VN, vs. the control condition 3 months later without any stimulation. Signal increases in the brainstem and cerebellum were more pronounced in the patients with left-sided VN located in the posterior ponto-mesencephalic brainstem and cerebellum bilaterally ($p \leq 0.001$ uncorrected)

Pooled data of patients with right- and left-sided VN gave the following results (Fig. 3): a positive correlation with the metabolism for the retroinsular region, posterior insula merging into the parahippocampal gyrus bilaterally, right more than left (right VOI 5: 557 voxels, $T = 3.12$; left VOI 6: 145 voxels, $T = 3.63$), as well as for the inferior/medial temporal gyrus (BA 46, 10) bilaterally, on the right side merging into the anterior insula ($T = 3.74$; $R^2 = 0.36$) and for the right precuneus (BA 7; $T = 3.28$; $R^2 = 0.30$). Small positively correlated areas were found in the precentral gyrus (BA 6, 20 voxels) and left middle frontal gyrus (BA 8, 37 voxels). These areas mainly represent multisensory vestibular cortex regions.

A negative correlation was observed for the medial part of the superior frontal gyrus (BA 6, 9) and anterior cingulum (BA 32) ($T = 5.63$; $R^2 = 0.56$), containing the supplementary eye fields bilaterally, as well as for the left superior temporal gyrus (BA 22), which merges into the adjacent anterior insula and upwards into parts of the

Fig. 3 Correlation analyses of the glucose metabolism with the latency between disease onset and PET measurement, the deviation of the subjective visual vertical (SVV) as a sign of tonic vestibular dysfunction in the acute stage, and the slow-phase velocity of the spontaneous nystagmus (SPN) in the acute stage in left- and right-sided VN. **a** shows representative brain slices (positively correlated areas are indicated in *red*; negative in *blue*), **b** the regression plots and R^2 values for the maximum voxel within the volumes of interest (VOIs; *red circles*). In the pooled data, positive correlations with the latency to the first PET scan were found for the lingual gyrus (VOI 1) and the precuneus (VOI 2), negative correlations for the upper medial parts of the middle frontal gyrus (frontal eye field) bilaterally (VOI 3 and 4), the lower middle frontal gyrus, and the left postcentral gyrus. Pooled data of patients with right- and left-sided VN showed positive correlations with the deviation of the SVV mainly for the retroinsular regions bilaterally (VOI 5 and 6), right more than left. Negative correlations were seen for the medial part of the superior frontal gyrus, anterior cingulum bilaterally, the left superior temporal gyrus and adjacent anterior insula, as well as the superior and middle frontal gyri bilaterally covering the prefrontal cortex and frontal eye field (VOI 7 and 8). In patients with right-sided VN, positive correlations with the slow phase velocity of SPN were located in the anterior insula bilaterally (VOI 9 and 10), the left posterior insula (VOI 11), middle temporal gyrus, and the inferior frontal gyrus/precentral gyrus. Patients with left-sided VN showed positive correlations for the left middle frontal/precentral gyrus (frontal eye field; VOI 12), the left inferior parietal lobule, and precuneus, all of which are oculomotor and multisensory vestibular cortex areas ▶

inferior, superior, and middle frontal as well as precentral gyrus (BA 6, 8, 9), covering the prefrontal cortex and the left frontal eye field (Fig. 3, VOI 7: $T = 5.65$). On the right side these cortical eye fields within the inferior/middle frontal gyrus/precentral gyrus (BA 6, 9; VOI 8: $T = 3.47$) as well as the superior frontal gyrus (BA 8) showed separate clusters. Thus, negative correlations were found between glucose metabolism and the different cortical oculomotor areas (eye fields) bilaterally.

Caloric hypo- or unresponsiveness

The pooled data showed a positive correlation of the amount of vestibular malfunction (due to caloric hypo- or unresponsiveness) with the glucose metabolism for the precentral gyrus bilaterally (BA 6; right: $T = 4.43$; left: $T = 3.93$; $R^2 = 0.50$), and the left middle temporal gyrus (BA 21; $T = 3.35$). Both reflect oculomotor areas (not shown). Negative correlation analyses yielded no significant results.

Latency (in days) between symptom onset and first PET

Pooled data showed a negative correlation with the glucose metabolism bilaterally for the upper medial parts of the middle frontal gyrus (BA 8, frontal eye field: right: $T = 3.63$; left: $T = 3.63$; Fig. 3, VOI 3 and 4) bordering the anterior cingulate gyrus (BA 32, 24), and the lower lateral middle frontal gyrus (BA 9, 46, 10) as well as for the left inferior parietal lobule/postcentral gyrus (BA 40,

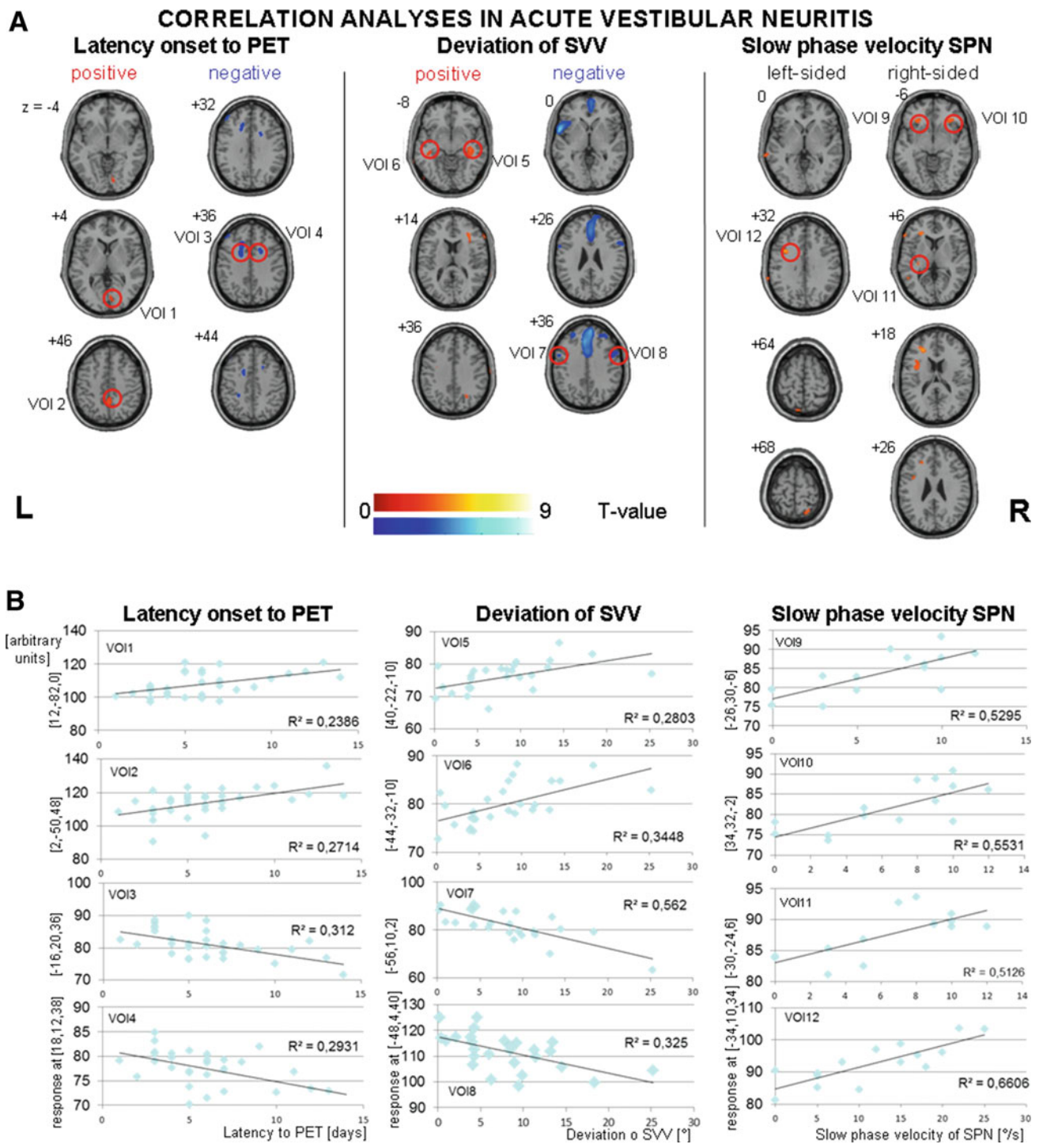

parietal eye field/somatosensory cortex; $T = 3.06$). Positive correlations were seen for the right visual cortex (lingual gyrus, BA 17, 18; $x, y, z = 12, -82, 0$; VOI 1: $T = 3.02$) and precuneus (BA 7; $x, y, z = 2, -50, 48$; VOI 2: $T = 3.29$). This means that the shorter the time interval after disease onset, the stronger the activations within the frontal eye field, prefrontal cortex, and the inferior parietal lobule (compatible with stronger spontaneous nystagmus). The longer the time interval, the more glucose metabolism within the visual cortex, i.e., the deactivations within the visual cortex decreased.

The recalculations of the regression analyses adding age and gender as covariates confirmed the given results: all relevant reported areas were seen again; only the *T*-values and coordinates of the maximum voxel as well as the cluster sizes differed slightly.

Multigroup statistical analyses

The multigroup statistical analyses (A) (VN right acute–chronic phase) vs. (VN left acute–chronic phase) and (B) (VN right chronic–acute phase) vs. (VN left chronic–acute phase) gave no significant results for the analyses of the total patients. In the most severe cases the contrast A gave only one area in the anterior cingulate gyrus (BA 24/32); the contrast B gave two small clusters in the left upper anterior cingulate gyrus (BA 24) and at the end of the right central sulcus post centrally (BA 45).

Group comparisons with healthy controls at rest

The analyses of VN right in the acute phase vs. the controls at rest gave significant clusters in the frontal eye fields bilaterally (middle frontal gyrus, BA 8), the right central ponto-mesencephalic brainstem merging into the adjacent temporal lobes, and the left thalamus. The inverse contrast of healthy controls vs. VN right showed bilateral signal differences, due to CMRglc decreases in the acute phase, in the visual cortex bilaterally (cuneus, lingual, middle and inferior occipital gyri; BA 17, 18, 19), including lower parts of the right precuneus.

Clusters found in the contrast VN left acute phase vs. controls at rest were mainly in the ponto-mesencephalic brainstem, and additional smaller areas in the basal ganglia and the cerebellum bilaterally. In the inverse contrast, signal decreases occurred primarily in the right visual and somatosensory cortex (postcentral gyrus).

The results of the comparison of patient data with that of healthy controls at rest—the latter were used to substitute for the baseline condition (which was not available in patients)—showed similar patterns (signal increases in temporo-parietal and oculomotor areas in the contrast patient PET A vs. healthy controls, and signal decreases in visual and somatosensory cortex areas in the contrast healthy controls vs. patient PET A) to those found in the subtraction analyses of patients, which compared acute and chronic phases (contrast A vs. B and vice versa). These results allow the interpretation that the signal changes in the temporo-parietal regions reflect signal *increases* ("activations") in the acute phase of VN, and in the occipital cortex signal *decreases* ("deactivations") in the acute phase of VN. The values derived from three-dimensional stereotactic surface projections in single patients who had already shown glucose hypermetabolism in temporo-parietal vestibular areas, and glucose hypometabolism in visual cortex areas also supports this interpretation.

Discussion

The major finding of this FDG-PET study in right- and left-sided VN showed differential effects on the activation–deactivation pattern in the acute stage of disease. Compared to the symptom-free stage 3 months later, these differences can be attributed to the underlying organizational asymmetries of the central vestibular system present in normal subjects, i.e., the dominance of ipsilateral pathways and the right hemisphere in right-handers (Dieterich et al. 2003; Bense et al. 2003).

Patients with right- or left-sided VN showed an up-regulation of glucose metabolism within the central vestibular system and simultaneously a down-regulation of glucose metabolism in the visual and somatosensory cortices in the analysis of the contrast acute vs. chronic phase. Thus, the reciprocal interaction between the two sensory cortices, visual and vestibular, shown earlier (Brandt et al. 1998), is preserved. The activated areas were preferably the *contralateral* parieto-insular vestibular cortex and the posterolateral thalamus, hippocampus, anterior cingulate gyrus and the ponto-mesencephalic brainstem—all belong to the vestibular network. This means that the patterns were mirror-imaged for right- vs. left-sided lesions. Changes in activation appeared to be most pronounced in patients with more severe vestibular deficits and with right-sided VN. The latter is best explained by the missing "dominant" ipsilateral input to the vestibular cortex of the dominant right hemisphere. However, multigroup subtraction analyses that statistically compare right- and left-sided VN did not yield any significant results. This might be due to the fact that both groups elicited similar bilateral patterns that differ only in their weighting for each hemisphere.

No signal changes were found in areas outside the vestibular, visual, and somatosensory networks, suggesting that central vestibular compensation in acute peripheral lesions is mainly achieved within the known cortical visual–vestibular–oculomotor networks, and other areas are not used. This is of particular importance, since cross-modal plasticity due to reorganization of cortical processing during acoustic and tactile stimuli has been demonstrated in visually deprived patients (Théoret et al. 2004; Collignon et al. 2009; Ptito et al. 2012). For example, in visually deprived patients increases in visual cortex areas were found during acoustic stimulation. The absence of cross-modal activation after unilateral vestibular loss can be explained by the fact that each labyrinth (namely the intact one) supplies the bilateral vestibular cortex.

The concurrent down-regulations of glucose metabolism in the visual and somatosensory cortices after unilateral vestibular loss were side-specific for right- and left-sided lesions. They were stronger for right-sided VN and in patients with more severe vestibular deficits in the acute phase. An additional up-regulation of glucose metabolism was found within the cerebellar vermis and hemispheres bilaterally of left-sided VN, which hypothetically is related to mechanisms of central compensation that seem to

depend on side effects in the sensorial weight (i.e., dominance) of right-sided pathways.

Vestibular tonus imbalance due to unilateral loss

The asymmetry of cortical activations within the contralateral vestibular network can be attributed to the depression of the more dominant ipsilateral right ascending projections to the right hemisphere with a right-sided peripheral vestibular loss. Thus, the tonus imbalance at the vestibular nuclei level mimics a left-sided vestibular excitation by increasing the resting discharge rate in the unaffected left vestibular nucleus complex. This effect is weaker for left-sided lesions. These differential effects of left- and right-sided lesions are also reflected in the current pontine and mesencephalic brainstem activations, findings supported by recent animal data on vestibular compensation after unilateral labyrinthine deafferentation in rats and frogs. The vestibular neuronal excitability and the molecular mechanisms of neural and synaptic plasticity in the vestibular nuclei showed rapid compensatory changes, e.g., in GABA receptor efficacy in the medial vestibular nucleus neurons (Yamanaka et al. 2000; Guilding and Dutia 2005). A down-regulation in the ipsilateral and a simultaneous up-regulation in the contralateral vestibular nucleus neurons result. Furthermore, inhibitory commissural fibers become fewer, whereas excitatory commissural inputs expand (Goto et al. 2001; Dieringer 2003).

Patients with left-sided VN have additional up-regulations of the glucose metabolism in the cerebellar hemispheres and vermis bilaterally (accentuated in the most severe cases), which is not found in right-sided VN. One can speculate that compensation in patients with left-sided lesions, which affects the weaker ascending cortical projection and thereby attenuates vestibular activity of the unaffected dominant right side, is mainly achieved by readjusting the imbalance at vestibular nuclei level via infratentorial ponto-cerebellar loops (Barmack 2003). In contrast, compensation in right-sided lesions, which affect the "dominant" ascending cortical projection, preferably involves thalamo-cortical mechanisms for central compensation.

Correlation analyses between glucose metabolism and vestibular and oculomotor parameters

The severity of vestibular dysfunction in the acute phase is indicated by different neurophysiological parameters, e.g., the slow-phase velocity of spontaneous nystagmus, the tilts of the subjective visual vertical, and the caloric hypo- or unresponsiveness, all of which served as correlation parameters. First, the slow-phase velocity of spontaneous nystagmus during the acute stage of VN correlated positively with the glucose metabolism in vestibular and oculomotor areas of the parieto-temporal cortex and the frontal eye fields. Second, the index of vestibular failure, i.e., the caloric asymmetry between the affected and unaffected ears, correlated positively with bilateral oculomotor areas. Third, the signs of vestibular graviceptive deficit as measured by subjective visual vertical correlated positively with the glucose metabolism for the posterior insula and retroinsular region bilaterally, right more than left, the medial temporal gyrus bilaterally, and also areas that represent early multisensory vestibular cortex regions responsible for the perception of verticality (Baier et al. 2012). In addition, the pooled data of left- and right-sided VN gave evidence that the latency until the first PET was performed correlated positively with the glucose metabolism in the visual cortex and negatively with that in the frontal eye field and the inferior parietal lobule. This means, the sooner PET is performed (strong spontaneous nystagmus), the more activity there is in areas of the vestibular and oculomotor networks.

The different correlation analyses gave further insights into separate functions within the cortical vestibular–oculomotor network, thus reflecting the severity and acuity of an acute unilateral peripheral loss. These correlation analyses confirmed and extend the results of the pilot study in five right-sided VN (Bense et al. 2004) as well as the data on healthy subjects during galvanic vestibular (Stephan et al. 2005) or visual motion stimulation inducing circular vection (Bense et al. 2012). These studies were able to attribute certain aspects of the applied stimulus, such as stimulus intensity, frequency, or duration to particular parts of the network. Interestingly, the results of the current study agreed with those results and remained unaffected by the addition of age and gender as covariates to the regression analyses. This agrees with clinical experience that the course of VN can vary in women and men as well as in younger or older adults, independently of their measurable vestibular deficit.

In summary, the mechanism of central compensation in unilateral vestibular failure is based on a shift of the dominant ascending vestibular input from the ipsilateral to the contralateral pathways. Because of the dominance of the right-sided ascending pathways and the dominance of the right hemisphere in right-handers, this shift will be more pronounced for right-sided than for left-sided peripheral vestibular lesions.

Acknowledgments The work was supported by the German Research Foundation (Deutsche Forschungsgemeinschaft: Di 379/4-3/4), the Foundation "Stiftung Rheinland-Pfalz für Innovation" (961-386261/759), the BMBF (01 GW 0642), and the Hertie-Foundation. Dr. Dieterich, Dr. Bartenstein, Dr. Brandt receive research support from Bundesministerium für Bildung und Forschung (BMBF). Dr. Dieterich serves on the editorial board of *Annals of Neurology* and

received research support from Deutsche Forschungsgemeinschaft. Dr. Brandt receives support from the Hertie-Foundation. Dr. Becker-Bense, Mr. Buchholz, Dr. Schreckenberger report no disclosures.

References

Akbarian S, Grüsser OJ, Guldin WO (1994) Corticofugal connections between the cerebral cortex and brainstem vestibular nuclei in the macaque monkey. J Comp Neurol 339:421–437

Baier B, Suchan J, Karnath HO, Dieterich M (2012) Neural correlates of disturbed perception of verticality. Neurology 78:728–735

Baloh RW (2003) Clinical practice. Vestibular neuritis. N Engl J Med 348:1027–1032

Barmack NH (2003) Central vestibular system: vestibular nuclei and posterior cerebellum. Brain Res Bull 60(5–6):511–541

Bartenstein P, Minoshima S, Hirsch C, Buch K, Willoch F, Mosch D, Schad D, Schwaiger M, Kurz A (1997) Quantitative assessment of cerebral blood flow in patients with Alzheimer's disease by SPECT. J Nucl Med 38:1095–1101

Bartenstein P, Asenbaum S, Catafau A, Halldin C, Pilowski L, Tatsch K (2002) European association of nuclear medicine procedure guidelines for brain imaging using F-18 FDG. Eur J Nucl Med 29:43–48

Bartlett EJ, Brodie JD, Wolf AP, Christmas DR, Laska E, Meissner M (1988) Reproducibility of cerebral glucose metabolic measurements in resting human subjects. J Cereb Blood Metab 8(4):502–512

Bense S, Stephan T, Yousry TA, Brandt T, Dieterich M (2001) Multisensory cortical increases and decreases during vestibular galvanic stimulation (fMRI). J Neurophysiol 85:886–899

Bense S, Bartenstein P, Lutz S, Stephan T, Schwaiger M, Brandt Th, Dieterich M (2003) Three determinants of vestibular hemispheric dominance during caloric stimulation. Ann N Y Acad Sci 1004:440–445

Bense S, Bartenstein P, Lochmann M, Schlindwein P, Brandt T, Dieterich M (2004) Metabolic changes in vestibular and visual cortices in acute vestibular neuritis. Ann Neurol 56:624–630

Bense S, Buchholz HG, Zu Eulenburg P, Best C, Bartenstein P, Schreckenberger M, Dieterich M (2012) Ventral and dorsal streams processing visual motion perception (FDG-PET study). BMC Neurosci. doi:10.1186/1471-2202-13-81

Brandt T, Dieterich M (1994) Vestibular syndromes in the roll plane: topographic diagnosis from brainstem to cortex. Ann Neurol 36:337–347

Brandt T, Bartenstein P, Janek A, Dieterich M (1998) Reciprocal inhibitory visual–vestibular interaction. Visual motion stimulation deactivates the parieto-insular vestibular cortex. Brain 121:1749–1758

Chen A, DeAngelis GC, Angelaki DE (2010) Macaque parieto-insular vestibular cortex: responses to self-motion and optic flow. J Neurosci 30:3022–3042

Collignon O, Voss P, Lassonde M, Lepore F (2009) Cross-modal plasticity for the spatial processing of sound in visually deprived subjects. Exp Brain Res 193:343–358

Curthoys IS, Halmagyi GM (1994) Vestibular compensation: a review of the oculomotor, neural, and clinical consequences of unilateral vestibular loss. J Vest Res 5:67–107

Dieringer N (2003) Activity-related postlesional vestibular reorganization. Ann N Y Acad Sci 1004:50–60

Dieterich M, Bense S, Lutz S, Drzezga A, Stephan T, Brandt T, Bartenstein P (2003) Dominance for vestibular cortical function in the non-dominant hemisphere. Cereb Cortex 13:994–1007

Emri M, Kisely M, Lengyel Z, Balkay L, Marian T, Miko L, Berenyi E, Sziklai I, Tron L, Toth A (2003) Cortical projection of peripheral vestibular signaling. J Neurophysiol 89:2639–2646

Fasold O, von Brevern M, Kuhberg M, Ploner CJ, Villringer A, Lempert T, Wenzel R (2002) Human vestibular cortex as identified with caloric stimulation in functional magnetic resonance imaging. NeuroImage 7(3):1384–1393

Friston KJ, Frith CD, Liddle PF et al (1990) The relationship between global and local changes in PET scans. Hum Brain Mapp 13:1038–1040

Friston KJ, Asburner J, Frith CD et al (1995a) Spatial registration and normalization of images. Hum Brain Mapp 2:165–189

Friston KJ, Holmes AP, Worsley KJ et al (1995b) Statistical parametric maps in functional imaging: a general linear approach. Hum Brain Mapp 2:189–210

Gispert JD, Pascau J, Reig S, Martínez-Lázaro R, Molina V, García-Barreno P, Desco M (2003) Influence of the normalization template on the outcome of statistical parametric mapping of PET scans. NeuroImage 19:601–612

Goto F, Straka H, Dieringer N (2001) Postlesional vestibular reorganization in frogs: evidence for a basic reaction pattern after nerve injury. J Neurophysiol 85(6):2643–6246

Guilding C, Dutia MB (2005) Early and late changes in vestibular neuronal excitability after deafferentation. NeuroReport 16:1415–1418

Guldin WO, Grüsser OJ (1996) The anatomy of the vestibular cortices of primates. In: Collard M, Jeannerod M, Christen Y (eds) Le cortex vestibulaire. Editions IRVINN, Ipsen, pp 17–26

Halmagyi GM, Weber KP, Curthoys IS (2010) Vestibular function after acute vestibular neuritis. Restor Neurol Neurosci 28(1): 37–46

Honrubia V (1994) Quantitative vestibular function tests and the clinical examination. In: Herdman SJ (ed) Vestibular rehabilitation. Davis, Philadelphia, pp 113–164

Jongkees LBW, Maas JPM, Philipszoon AJ (1962) Clinical nystagmography: a detailed study of electro-nystagmography in 341 patients with vertigo. Pract Otorhinolaryngol 24:65–93

Kleinschmidt A, Thilo KV, Büchel C, Gresty MA, Bronstein AM, Frackowiak RSJ (2002) Neuronal correlates of visual-motion perception as object- or self-motion. NeuroImage 16:873–882

Laurienti PJ, Burdette JH, Wallace MT, Yen YF, Field AS, Stein BE (2002) Deactivation of sensory-specific cortex by cross-modal stimuli. J Cogn Neurosci 14:420–429

Lobel E, Kleine JF, Le Bihan D, Leroy-Willig A, Berthoz A (1998) Functional MRI of galvanic vestibular stimulation. J Neurophysiol 80:2699–2709

Lumer ED, Friston KJ, Rees G (1998) Neural correlates of perceptual rivalry in the human brain. Science 280:1930–1934

Maihöfner C, Handwerker HO, Birklein F (2006) Functional imaging of allodynia in complex regional pain syndrome. Neurology 66(5):711–717

Mast FW, Merfeld DM, Kosslyn SM (2006) Visual mental imagery during caloric vestibular stimulation. Neuropsychologia 44(1): 101–109

Merabet LB, Swisher JD, McMains SA, Halko MA, Amedi A, Pascual-Leone A, Somers DC (2007) Combined activation and deactivation of visual cortex during tactile sensory processing. J Neurophysiol 97:633–1641

Miyamato T, Fukushima K, Takada T, de Waele C, Vidal PP (2007) Saccular stimulation of the human cortex: a functional magnetic resonance imaging study. Neurosci Lett 423(1):68–72

Naidich TP, Brightbill TC (2003) Vascular territories and watersheds: a zonal frequency analysis of the gyral and sulcal extent of cerebral infarcts. Part I: the anatomic template. Neuroradiology 45:536–540

Naito Y, Tateya I, Hirano S, Inoue M, Funabiki K, Toyoda H, Ueno M, Ishizu K, Nagahama Y, Fukuyama H, Ito J (2003) Cortical correlates of vestibulo-ocular reflex modulation: a PET study. Brain 126:1562–1578

Oldfield RC (1971) The assessment and analysis of handedness: the Edinburgh inventory. Neuropsychologia 9:97–113

Ptito M, Matteau I, Zhi Wang A, Paulson OB, Siebner HR, Kupers R (2012) Crossmodal recruitment of the ventral stream in congenital blindness. Neural Plat. doi:10.1155/2012/304045

Schlindwein P, Mueller M, Bauermann T, Brandt T, Stoeter P, Dieterich M (2008) Cortical representation of saccular vestibular stimulation: VEMPs in fMRI. NeuroImage 39(1):19–31

Stephan T, Deutschländer A, Nolte A, Schneider E, Wiesmann M, Brandt T, Dieterich M (2005) Functional MRI of galvanic vestibular stimulation with alternating currents at different frequencies. Neuroimage 26:721–732

Talairach J, Tournoux P (1988) Co-planar Stereotaxic Atlas of the Human Brain. Georg Thieme Verlag, Stuttgart

Théoret H, Merabet L, Pasqual-Leone A (2004) Behavioural and neuroplastic changes in the blind: evidence for functionally relevant cross-modal interactions. J Physiol Paris 98:221–233

Wenzel R, Bartenstein P, Dieterich M, Danek A, Weindl A, Minoshima S, Ziegler S, Schwaiger M, Brandt T (1996) Deactivation of human visual cortex during involuntary ocular oscillations. A PET activation study. Brain 119:101–110

Wienhard K, Eriksson L, Grootoonk S, Casey M, Pietrzyk U, Heiss WD (1992) Performance evaluation of the positron scanner ECAT EXACT. J Comput Assist Tomogr 16:804–813

Worsley KJ, Evans AC, Marrett S, Neelin P (1992) A three-dimensional statistical analysis for CBF activation studies in human brain. J Cereb Blood Flow Metab 12:900–918

Yamanaka T, Him A, Cameron SA, Dutia MB (2000) Rapid compensatory changes in GABA receptor efficacy in rat vestibular neurons after unilateral labyrinthectomy. J Physiol 523:413–424

Yousry TA, Schmid UD, Alkadhi H, Schmidt D, Peraud A, Büttner A, Winkler P (1997) Localization of the motor hand area to a knob on the precentral gyrus. A new landmark. Brain 120:141–157

Zu Eulenburg P, Caspers S, Roski C, Eickhoff SB (2012) Meta-analytical definition and functional connectivity of the human vestibular cortex. Neuroimage 60:162–169